Hindawi Publishing Corporation
Journal of Engineering
Volume 2013, Article ID 898634, 7 pages
http://dx.doi.org/10.1155/2013/898634

Research Article

Dynamic Modeling and Simulation of a Super-High-Speed Circumferential-Flux Hysteresis Motor

A. Halvaei Niasar,[1] M. Zare,[1] and H. Moghbelli[2]

[1] *Faculty of Electrical and Computer Engineering, University of Kashan, P.O. Box 87317-51167, Kashan, Iran*
[2] *Department of Electrical Engineering, Yazd University, P.O. Box 89195-741, Yazd, Iran*

Correspondence should be addressed to A. Halvaei Niasar; halvaei@kashanu.ac.ir

Received 16 September 2012; Revised 11 December 2012; Accepted 11 December 2012

Academic Editor: Sheng-Rui Jian

Copyright © 2013 A. Halvaei Niasar et al. This is an open access article distributed under the Creative Commons Attribution License, which permits unrestricted use, distribution, and reproduction in any medium, provided the original work is properly cited.

There is an interest in super-high-speed motors in industry applications such as gyroscope, micro gas turbines, centrifuge, machine tool spindle drives, and information storage disk drives. This paper presents the dynamic performance characteristics of hysteresis motors using a Matlab/Simulink software. A nonlinear mathematical model based on a *d-q* axis theory in the rotor reference frame is applied to study the starting and synchronization processes of a hysteresis machine with a circumferential-flux-type rotor. The steady-state and transient responses of the motor to different changes such as the variation in the load torque are provided. The calculation method of the motor parameters in dynamic modeling based on a steady-state model of the motor is presented. The simulation results such as the current,the input power, and power factor are compared with some experimental results in steady-state condition.

1. Introduction

The hysteresis motor is a well-known type of electrical machines. Basically, it is a synchronous motor. However, in spite of synchronous motors, it has a stable performance at asynchronous conditions similar to the induction motors. It is often used for small power applications that needs a very smooth torque at high speeds such as gas centrifuges and gyroscopes. Developing new semihard magnetic materials leads to a higher power range for Hysteresis motors up to 0.5 hp. hysteresis motors have a constant torque from starting to synchronous frequency and their starting current is at most 150% rated current. Nonetheless, the cost of hysteresis motors is high due to the special material of the rotor's ring. Moreover, hysteresis motors have a low power factor less than 0.5 and efficiency as high as 75% that limits their applications [1].

The structure of hysteresis motors is similar to induction motor. Figure 1 shows a cross-section of a hysteresis motors. Its stator is considered to have a three-phase two poles with sinusoidal distributed winding. The rotor includes two parts: (i) a magnetic ring which is the basic element for torque providing and (ii) the inside part of the rotor that is made of a non-magnetic material that acts as a support for the magnetic ring. The starting of the motor is due to the hysteresis losses induced in the rotor. The starting current is at most 200% of its full load current that can pull into synchronism any load inertia coupled to its shaft.

In this paper, the dynamic performance of hysteresis motor is investigated. The steady-state model of hysteresis motors is explored in Section 2. Then a *d-q* model of the hysteresis motor is developed in a rotor reference frame. Finally, some simulation results under different conditions are presented and compared with some measured results.

2. Steady-State Model of the a Hysteresis Motor

The electric equivalent circuit of a hysteresis motor for the steady-state synchronous operation is shown in Figure 2, including the stator impedances and voltage source E_p. The effect of the rotor magnetic material is to produce a "hysteresis lag angle β" between the stator MMF and the resultant air gap flux density waveforms [1].

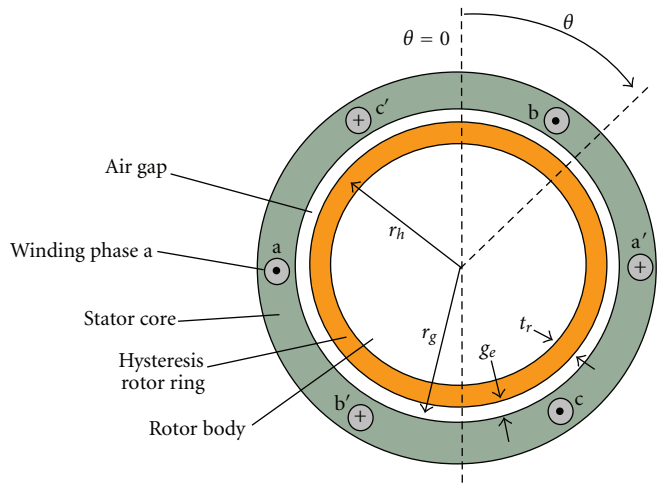

Figure 1: A cross-section of a circumferential-flux hysteresis motor.

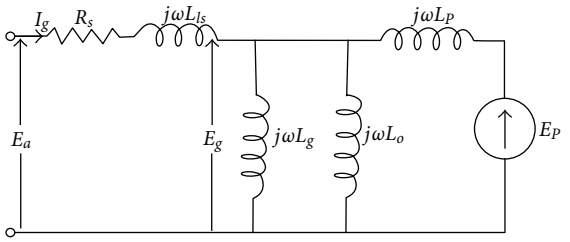

Figure 2: A equivalent circuit of a hysteresis motor based on an idealized B-H curve of a hysteretic material [1].

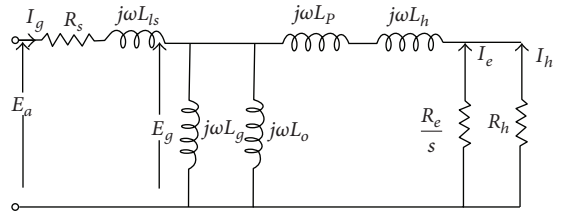

Figure 3: A steady-state equivalent circuit of a hysteresis motor.

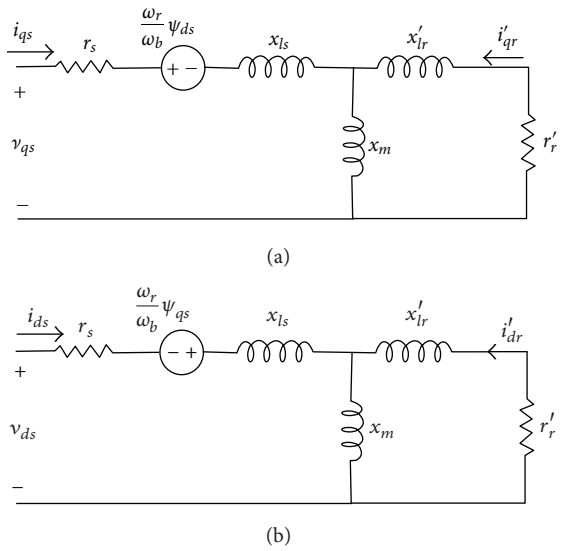

Figure 4: A hysteresis motor model in rotating *qd0* reference frame.

The values of air gap inductance L_g, unsaturated incremental inductance L_o and saturated incremental inductance L_p in Figure 2 are calculated from:

$$L_g = \frac{3\pi}{8}\frac{N_s^2\mu_o r_g l}{g_e},$$

$$L_o = \frac{3\pi}{8}\frac{N_s^2\mu_o\mu_{ro} t_r l}{r_h}, \quad (1)$$

$$L_p = \frac{3\pi}{8}\frac{N_s^2\mu_o\mu_p t_r l}{r_h},$$

where, N_s is the stator's winding turns, l is the axial length of stator or hysteresis ring, r_g is the mean radius of air gap, r_h is the mean radius of hysteresis ring on the rotor, t_r is the thickness of hysteresis ring, g_e is the effective width of air gap, μ_o is the free space permeability, μ_{ro} is the unsaturated relative permeability, and $\mu_p(=\mu_{rs}\|\mu_{ro})$ is the relative permeability with μ_{rs}as saturated relative permeability [1, 2].

The lag angle β is independent of the frequency of rotor magnetization but it depends on the shape of the hysteresis loop. At synchronous speed, the fundamental eddy current torque is zero and the operation of the motor is accomplished exclusively by the hysteresis torque that is developed from hysteresis power of B-H loop. The hysteresis power can be represented as hysteresis resistance R_h as function of lag angle. It can be approximated from the power loss approach as:

$$R_h = \frac{mE_g^2}{4B_r H_c f V_r}\sin\beta, \quad (2)$$

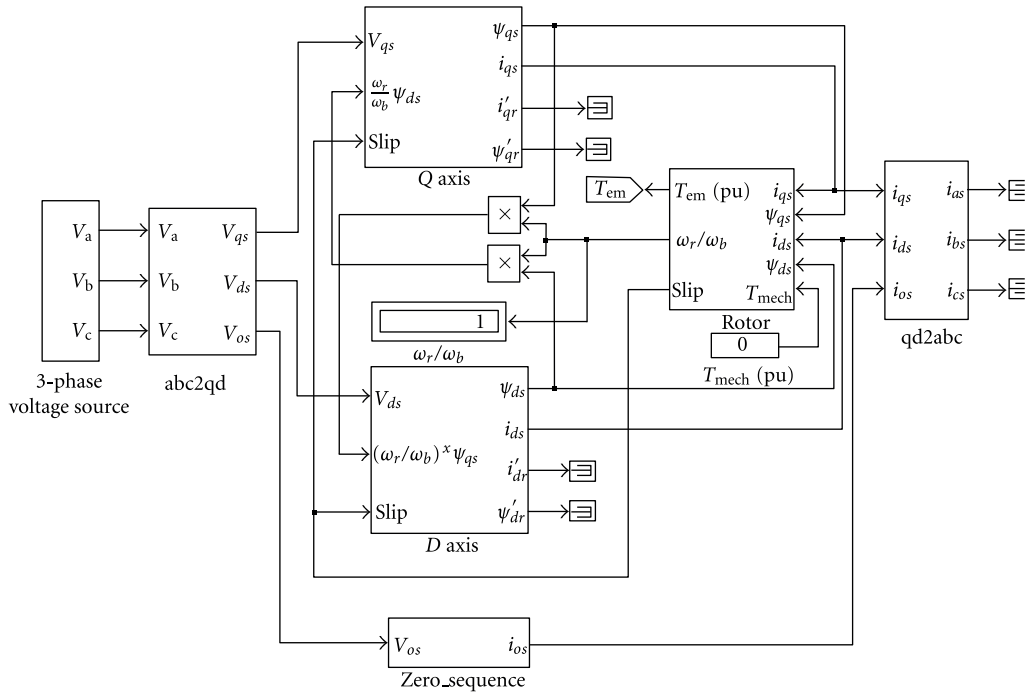

Figure 5: A dynamic modelling block diagram of a hysteresis motor in Simulink.

where, m is the number of phases, E_g is the air gap voltage, B_r and H_c are the residual flux density and coercive force of the hysteretic material, f is the supply frequency and V_r is the volume of hysteretic material.

At any speed except to synchronous speed, the motor torque is due to both the hysteresis and eddy current effects as shown in Figure 3. The representation of the rotor eddy current is carried out by equivalent resistance R_e as [2, 3]:

$$R_e = \frac{12\rho l}{10^4 A_h}, \tag{3}$$

where, ρ is the specific resistivity, and A_h is the cross sectional area of ring.

3. Dynamic Modeling of a Hysteresis Motor

Figure 4 shows the dynamic model of a hysteresis motor in *qd0* reference frame rotating with rotor speed ω_r. The difference between the model of hysteresis and general synchronous motors comes from the modeling of rotor materials that for the hysteresis motor is so different. For this purpose, the steady-state model of the rotor in hysteresis motors from Figure 3 is employed.

It is convenient to express the voltage and flux linkage equations in term of reactance rather than inductances [4, 5]. Hence, using $\psi = \omega_b \lambda$ the hysteresis motor voltage and linkage flux equations in the *qd0* rotating reference frame is represented by

$$\begin{aligned}
v_{qs} &= r_s i_{qs} + \frac{\omega_r}{\omega_b}\psi_{ds} + \frac{1}{\omega_b}\frac{d\psi_{qs}}{dt},\\
v_{ds} &= r_s i_{ds} - \frac{\omega_r}{\omega_b}\psi_{qs} + \frac{1}{\omega_b}\frac{d\psi_{ds}}{dt},\\
v'_{qr} &= 0 = r'_r i'_{qr} + \frac{d\psi'_{qr}}{dt},\\
v'_{dr} &= 0 = r'_r i'_{dr} + \frac{d\psi'_{dr}}{dt},\\
\psi_{qs} &= (x_{ls} + x_m) i_{qs} + x_m i'_{qr},\\
\psi_{ds} &= (x_{ls} + x_m) i_{ds} + x_m i'_{dr},\\
\psi'_{qr} &= x_m i_{qs} + (x'_{lr} + x_m) i'_{qr},\\
\psi'_{dr} &= x_m i_{ds} + (x_{ls} + x_m) i'_{dr},
\end{aligned} \tag{4}$$

where r_s is the stator coil resistance and x_{ls} is the stator leakage reactance. The quantities x_m and x'_{lr} are the magnetizing and rotor leakage reactance that are derived from the following:

$$\begin{aligned}
x_m &= (\omega L_g) \parallel (\omega L_o),\\
x'_{lr} &= \omega L_p + \omega L_h.
\end{aligned} \tag{5}$$

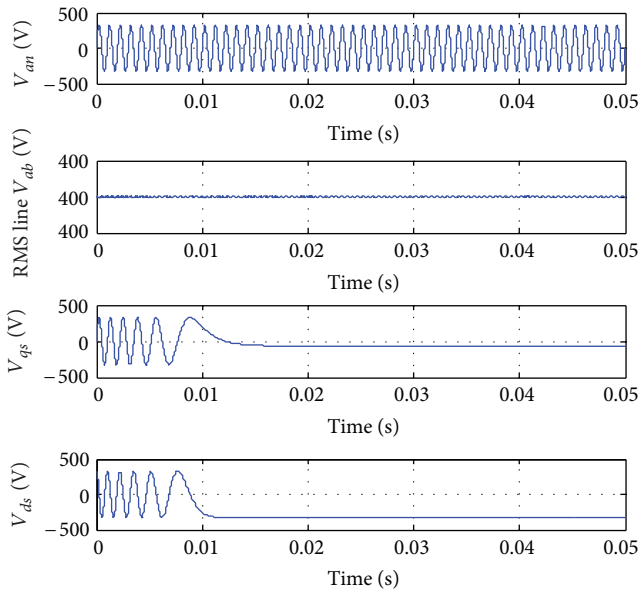

Figure 6: Stator voltage waveform at 60000 rpm at no-load condition.

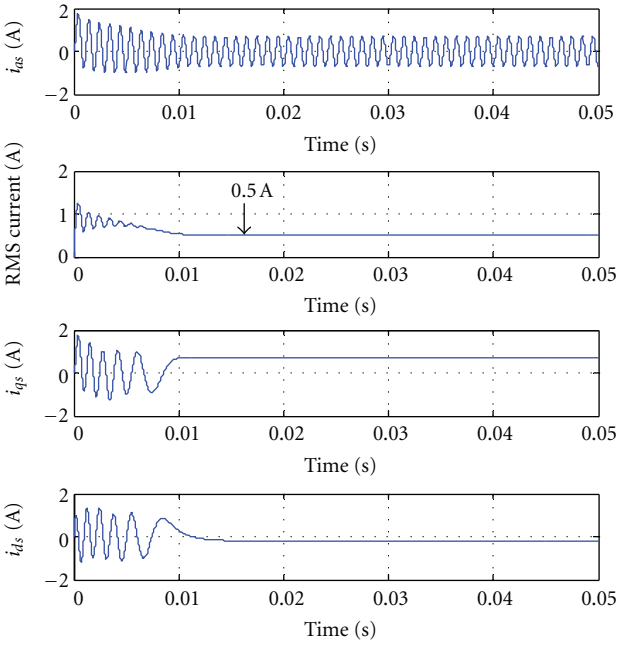

Figure 7: Stator current waveform at 60000 rpm at no-load condition.

The reactance ωL_h is the apparent reactance due to hysteresis ring and is approximated by

$$\omega L_h = \frac{R_h}{\tan \beta}, \tag{6}$$

And the rotor apparent resistance is given by

$$r_r^{'} = R_h \parallel \frac{R_e}{s} \tag{7}$$

Electromagnetic torque and the rotor speed are obtained from

$$T_{\text{em}} = \frac{3}{2}\frac{P}{2\omega_b}\left(\psi_{ds} i_{qs} - \psi_{qs} i_{ds}\right),$$
$$T_{\text{em}} - T_{mech} = \frac{2J}{P}\frac{d\omega_r(t)}{dt}, \tag{8}$$

where P is the number of stator poles and J is the shaft inertia moment. The definitions and corresponding values of the parameters for the employed hysteresis motor are listed in Table 1.

Table 1: Hysteresis motor parameters.

Number of poles	p	2
Rated output power	P	60 W
Rated voltage	V_s	400 V
Rated frequency	f_s	1000 Hz
Stator leakage reactance	X_{ls}	152 Ω/ph
Stator resistance	r_s	36 Ω/ph
Equivalent resistance due to eddy current	R_e	3288 Ω/ph
Equivalent resistance due to hysteresis ring	R_h	127 Ω/ph
Equivalent reactance due to hysteresis ring	X_h	163.7 Ω/ph
Unsaturated incremental reactance	X_o	451 Ω/ph
Saturated incremental reactance	X_p	13 Ω/ph
Air gap equivalent reactance	X_g	1217 Ω/ph

4. Simulation Results

The developed model has been simulated for a 60000 rpm super-high-speed hysteresis motor. The corresponding parameters are summarized in Table 1. Figure 5 shows the implementation of the dynamic modeling of hysteresis motors in Matlab/Simulink. Simulations are carried out at no-load and under full-load conditions.

Figure 6 shows the simulation results at a rated speed and at no-load condition. RMS value of the stator voltage is 400 volt. And the voltage waveform and its d-q components are shown. Figure 7 shows the instance and RMS value of the stator current as well as d-q components. The steady-state value of d-q components depend on the B-H curve of the rotor material (B_r and H_c). The RMS value of the stator current in steady state is 0.5 A. The transient time in simulation is about 0.01 sec. Figure 8 shows the variations of the developed torque, rotor speed and input power. There is no load on the rotor and so, the developed torque is zero at the steady state. The input power is equal to the stator copper loss.

Figure 9 shows the variations of the power factor, input active power, input reactive power, and available power of the motor at no-load condition. The power factor is too low, that is common in hysteresis motors. The input power is wasted in the winding of stator.

Figure 10 shows the variations of the motor quantities. Developed torque at the steady state reaches to 1 [pu].

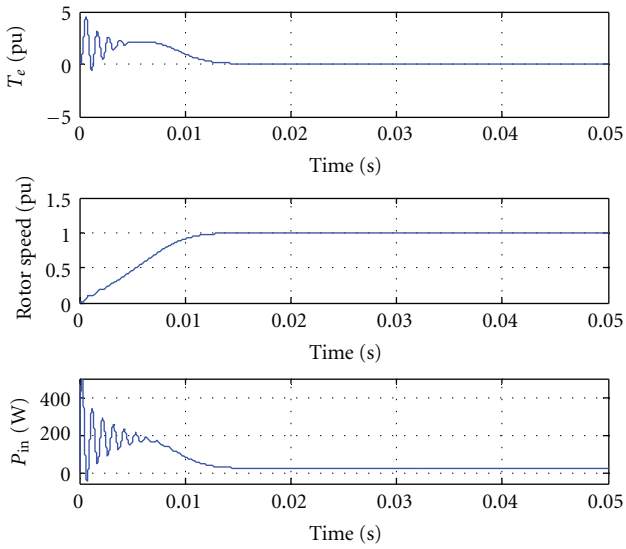

FIGURE 8: Torque/speed/input power at 60000 rpm at no-load condition.

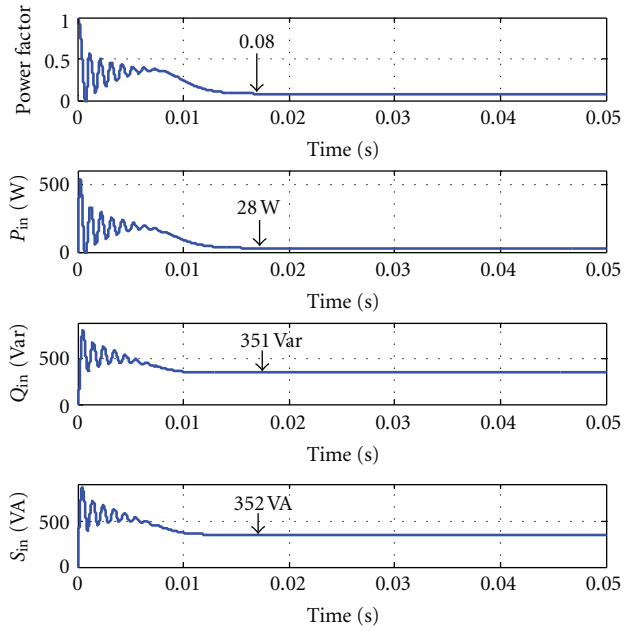

FIGURE 9: Power factor/P_{in}/Q_{in}/S_{in} at 60000 rpm at no-load condition.

The RMS value of the current is 0.53 [A] that is close to no-load current at the same conditions. Power factor grows up to 0.25 that confirms the power factor of the hysteresis motor is far from the power factor of PM and IM motors. The input active power is 91 [W] that is the summation of output power (60 W) and stator copper loss (31 W).

5. Experimental Results

In this section, some experimental results for a 60000 rpm hysteresis motor, under full-load condition at the steady

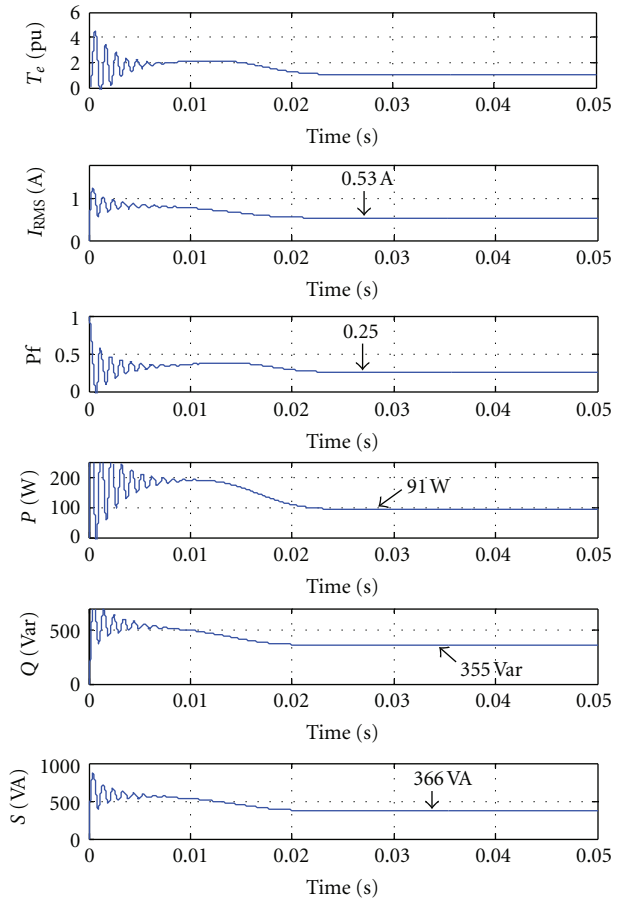

FIGURE 10: T_e/I_{rms}/Pf/P_{in}/Q_{in}/S_{in} at 60000 rpm under full-load condition.

state are presented. Due to some mechanical limitations and vibration at the starting process of the employed actual hysteresis motor, the starting process is carried out with a smooth ramp that it takes one hour time. So, because of the RAM limitation of the PC, the starting process has been simulated only for one second. Therefore, the simulated and measured results are compared just in steady state under full-load condition.

Figure 11 shows the current and voltage of the hysteresis motor which is fed from a high frequency PWM inverter. Moreover, one period of each waveform as well as corresponding fundamental harmonic are shown. An FFT analysis is carried out to identify the magnitude and frequency of the stator phase current and voltage. The magnitude of the stator current and voltage are close to the simulation results. To show the hunting phenomenon of hysteresis motor, the stator current and voltage are measured for one second in steady state. Figure 12 shows the instant RMS value of the current and voltage as well as the mean value of RMS during one second. The mean RMS value of the stator current and voltage are 0.55 A and 397 V, respectively, that confirms the simulation results. Moreover, variations of power factor and input power during one second are shown. The mean value of the power factor and power are 0.27 and 95 W, respectively,

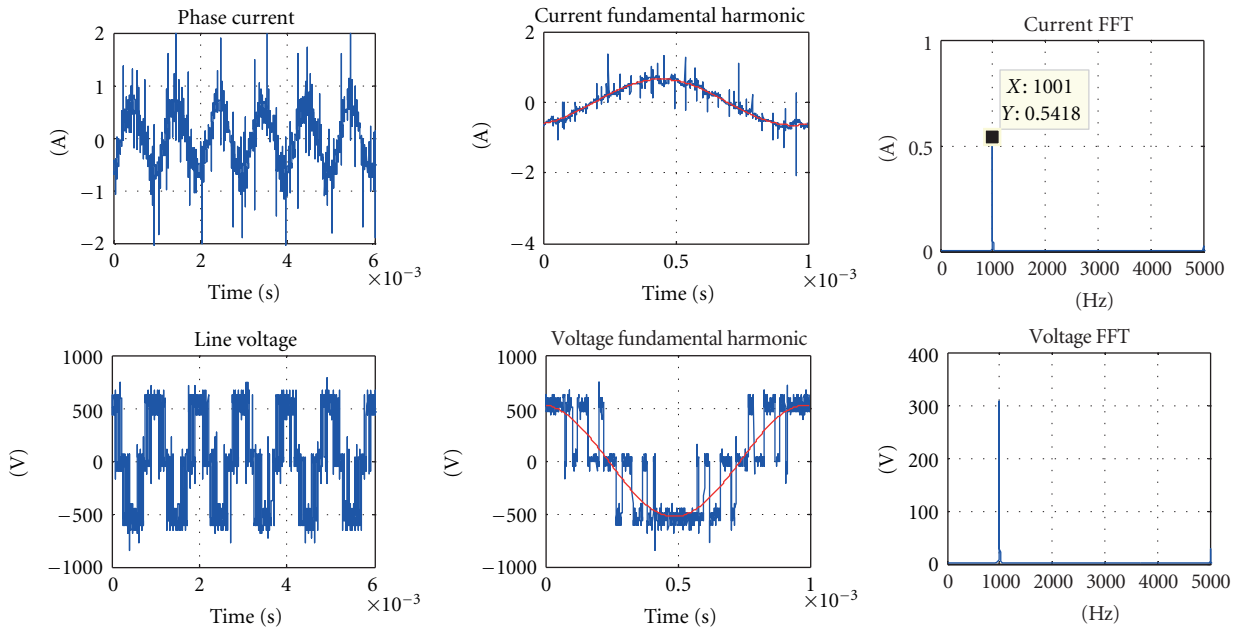

Figure 11: Experimental results and the FFT analysis of the stator current/voltage waveforms at 60000 rpm under full-load condition.

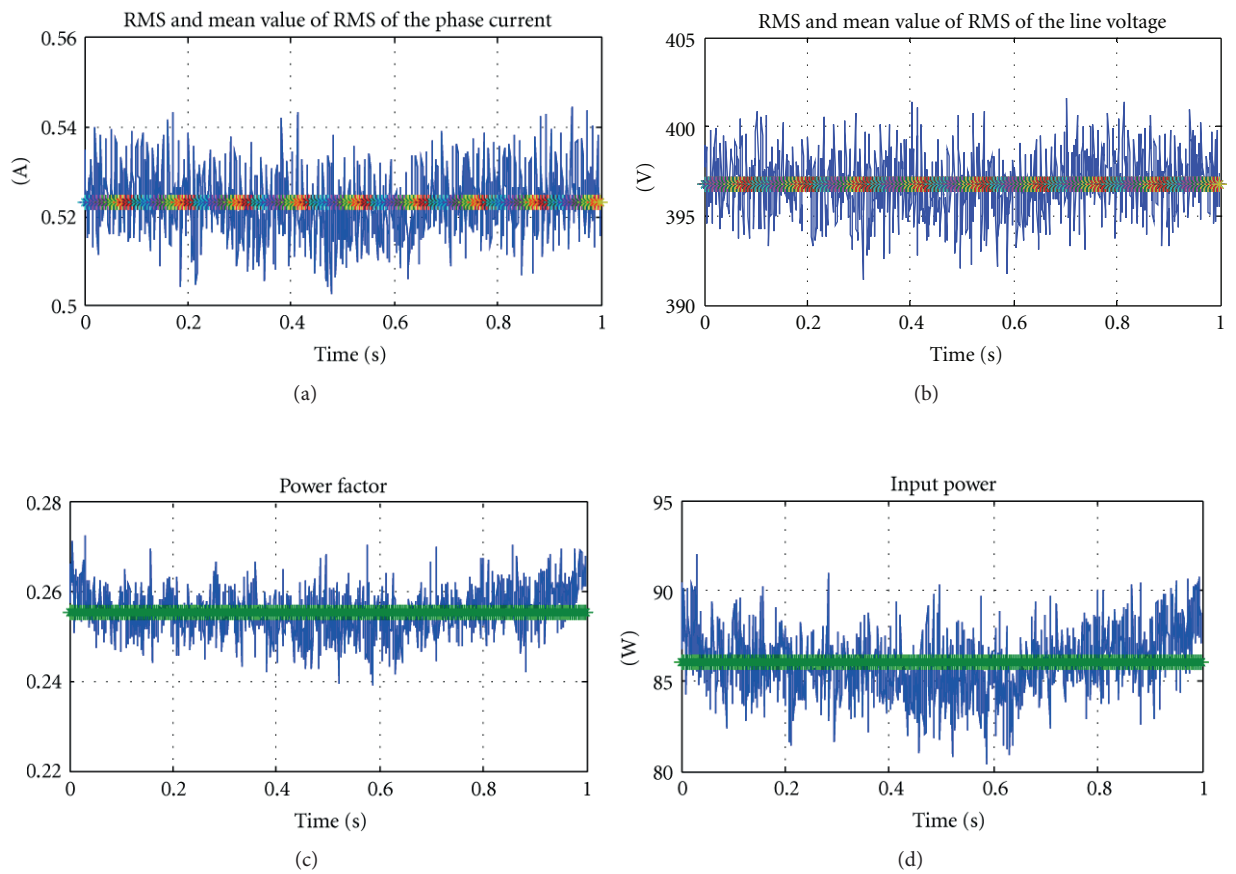

Figure 12: Experimental results of the stator current/voltage RMS value, power factor, and input power during 1 second.

whereas the corresponding simulated results are 0.25 and 91 W. There are a good agreement between simulation and experimental results.

6. Conclusion

A dynamic model for a circumferential-flux hysteresis motor has been developed and implemented in Simulink. A developed model is based on *d-q* theory and is similar to the model of the synchronous motor. The main point in the proposed model is the modeling of B-H characteristics of the hysteretic material of rotor and including in the dynamic model. There exists a close agreement between simulated and measured results. It is shown that the power factor of the motor is so low rather than PM or IM motors and the stator current does not have much change at no-load and full-load conditions. proposed model can easily be used for fault diagnosis, closed-loop vector control, sensorless control, and parameters identification.

References

[1] M. A. Copeland and G. R. Slemon, "An analysis of the hysteresis motor II—the circumferential flux machine," *IEEE Transactions on Power Apparatus and Systems*, vol. 83, no. 6, pp. 619–625, 1964.

[2] M. A. Rahman, "Analytical models for polyphase hysteresis motor," *IEEE Transactions on Power Apparatus and Systems*, vol. 92, no. 1, pp. 237–242, 1973.

[3] A. Darabi, H. Lesani, T. Ghanbari, and A. Akhavanhejazi, "Modeling and optimum design of disk-type hysteresis motors," in *Proceedings of the International Conference on Electrical Machines and Systems (ICEMS '07)*, pp. 998–1002, Shahrood, Iran, October 2007.

[4] C.-M. Ong, *Dynamic Simulations of Electric Machinery*, Prentice-Hall, 1998.

[5] M. A. Rahman and A. Osheibba, "Dynamic performance prediction of poly phase hysteresis motors," *IEEE Transactions on Industry Applications*, vol. 26, no. 6, pp. 1026–1033, 1990.

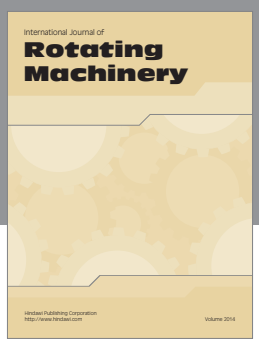

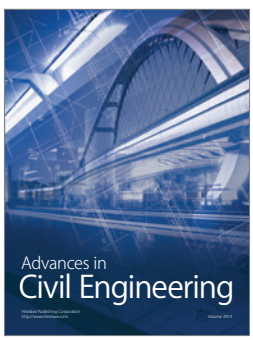

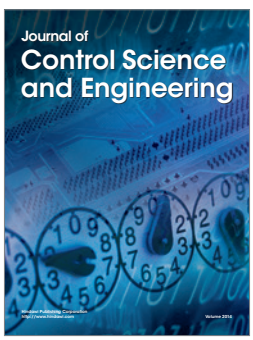

Hindawi
Submit your manuscripts at
http://www.hindawi.com